



LAWRENCE
LIVERMORE
NATIONAL
LABORATORY

Time-Space Position of Warm Dense Matter in Laser Plasma Interaction Process

L. F. Cao, I. Uschmann, E. Forster, F. Zamponi, T. Kampfer, A. Fuhrmann, A. Holl, R. Redmer, S. Toleikis, T. Tschentscher, O. L. Landen, S. H. Glenzer

November 15, 2006

Physics of Non-ideal Plasmas
Darmstadt, Germany
September 4, 2006 through September 8, 2006

Disclaimer

This document was prepared as an account of work sponsored by an agency of the United States Government. Neither the United States Government nor the University of California nor any of their employees, makes any warranty, express or implied, or assumes any legal liability or responsibility for the accuracy, completeness, or usefulness of any information, apparatus, product, or process disclosed, or represents that its use would not infringe privately owned rights. Reference herein to any specific commercial product, process, or service by trade name, trademark, manufacturer, or otherwise, does not necessarily constitute or imply its endorsement, recommendation, or favoring by the United States Government or the University of California. The views and opinions of authors expressed herein do not necessarily state or reflect those of the United States Government or the University of California, and shall not be used for advertising or product endorsement purposes.

Time-Space Position of Warm Dense Matter in Laser Plasma Interaction Process^a

L. F. Cao, I. Uschmann, E. Förster, F. Zamponi, T. Kämpfer, A. Fuhrmann,

Institute for Optics and quantum electronics, Friedrich-Schiller-University, Max-Wien-Platz 1,
D-07743 Jena, Germany

A. Höll, R. Redmer,

Institute for Physics, University Rostock, Universitätsplatz 3, D-18051 Rostock, Germany

S. Toleikis, T. Tschentscher,

Hasylab, DESY Hamburg, Notkestraße 85, D-22603 Hamburg, Germany

O. L. Landen, S. H. Glenzer

L-399, Lawrence Livermore National Laboratory, University of California, P.O. Box 808,
Livermore, CA 94551, USA

Abstract: Laser plasma interaction experiments have been performed using an fs Titanium Sapphire laser. Plasmas have been generated from planar PMMA targets using single laser pulses with 3.3 mJ pulse energy, 50 fs pulse duration at 800 nm wavelength. Electron density distributions of the plasmas in different delay times have been characterized by means of Nomarski Interferometry. Experimental data were cautiously compared with relevant 1D numerical simulation. Finally these results provide a first experience of searching for the time-space position of the so-called warm dense plasma in an ultra fast laser target interaction process. These experiments aim to prepare near solid-density

^a Email address: cao@ioq.uni-jena.de

plasmas for Thomson scattering experiments using the short wavelength free-electron laser FLASH, DESY Hamburg.

I. Introduction

Ultra short-pulse high-intensity laser interact with planar PMMA target had been suggested as a methodology to generate the so-called warm dense matter, which could provide a possible target for the proposed short wavelength Thomson scattering experiments what should be done at the FLASH vacuum ultraviolet free electron laser (VUV-FEL) facility at DESY in Hamburg [1]. The goal of these experiments is to verify a consistent many-particle theory for Thomson scattering in warm dense matter [2]. Plasma densities of $10^{21} \sim 10^{22} \text{ cm}^{-3}$ and plasma temperature of several eV will be required in these experiments for a detailed analysis of the shape of the expected scattering signal according to a previous work [3]. In this paper, we report our experimental work to search for the time-space position of these dense plasmas in an ultra-fast- laser interacting with planar PMMA target process. Numerical simulations were firstly calculated by using MED 103 [4] which it is a one dimensional Lagrangian hydrodynamic code. According to that results a series of experiments were designed and then performed on a Titanium Sapphire fs laser facility in our laboratory. Electron density lower than $2 \times 10^{20} \text{ cm}^{-3}$ of the laser-induced plasmas were measured by a modified time resolved Nomarski interferometer [5] with frequency-doubled probe light. The time-space position of the warm dense matters then was determined by the measured gradient tendency of the plasmas along the axis perpendicular to the target.

II. Numerical simulation of laser PMMA target interaction

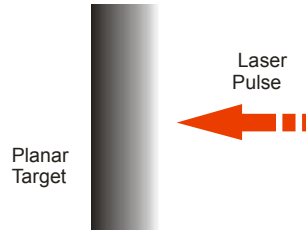


Figure 1 schematic for the calculation

Figure 1 shows the sketch for illustrating the laser target interaction in our calculation. An ultra short pulse laser irradiates perpendicular on a planar PMMA target and ablative plasmas are generated and evolve via time. This evolution can be calculated by using one-dimension hydrodynamic realistic code MED 103 [4] when providing all the parameters of the laser pulse what they are the wavelength, the energy, the duration and the pulse shape, the target parameters including the material, the density and the geometric configuration. The output of the code is a pack of time-space dependent plasma parameters including plasma density, plasma temperature, ionization state, pressure, and plasma velocity. The time resolved plasma density distribution and the plasma temperature distribution are of the most important interests here.

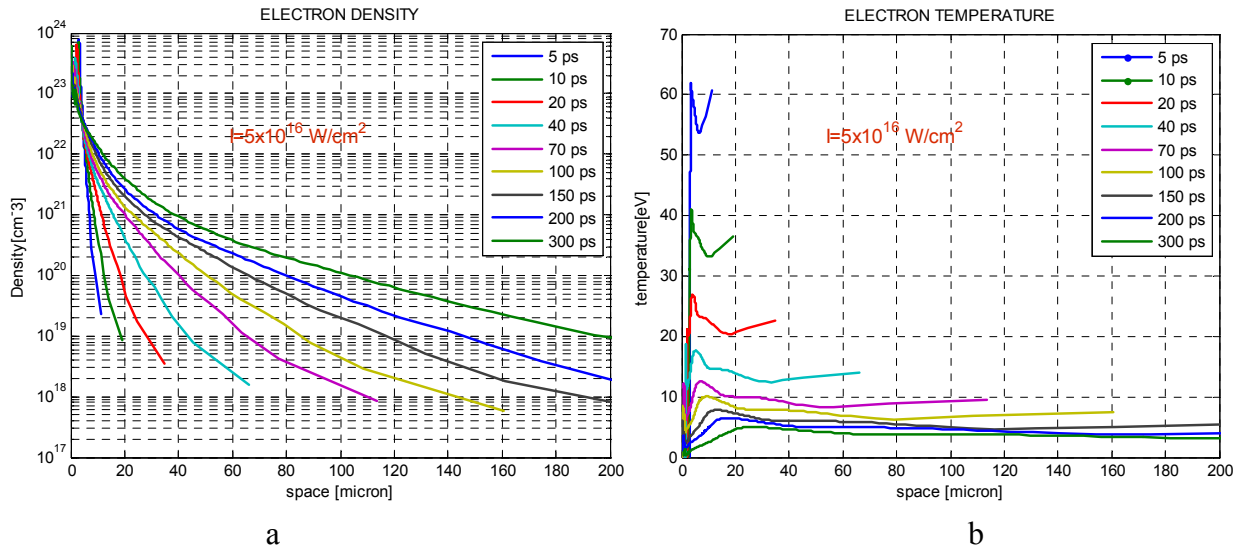


Figure 2. 1-D Numerical simulation result for laser PMMA planar target interaction. a) electron density profile; b) electron temperature profile along the axis. Laser parameter: $5 \times 10^{16} \text{ W/cm}^2$

Figure 2 shows the calculation results when choosing laser parameters as 800 nm wavelength, 50 fs pulse duration, $5 \times 10^{16} \text{ W/cm}^2$ intensity and Gaussian pulse shape. Very high density plasma ($> 7 \times 10^{23} \text{ cm}^{-3}$) with high temperature ($> 60 \text{ eV}$) was firstly generated on the target surface, and then expanded into and out of the target. The whole space that the plasmas occupied became larger and larger while the time proceeding. As a result, the electron density and the temperature decreased accompany with such a process. At a time point 300 ps after the laser shot, one can find that the expected warm dense matter with desired density and temperature emerged in a region bordered by the target and a plane 35 microns distant from the target.

Similar simulations for less intense laser were also calculated. Table I lists the region where the dense plasmas with densities of $10^{21} \sim 10^{22} \text{ cm}^{-3}$ existed and the relevant temperatures within these region at the point time point 300 ps after the laser shots. These data indicate that short-pulse laser with pulse duration of 100 fs, intensity less than 10^{14} W/cm^2 can nearly generate the desired warm dense matter, lasers with intensities of 10^{15} W/cm^2 and 10^{16} W/cm^2 can but the region where the warm dense matter exist were too close to the target. This means that it is impractical to generate the warm dense matter by laser beam with less intensity than 10^{16} W/cm^2 . Higher laser intensity than $5 \times 10^{16} \text{ W/cm}^2$ might be better, but it would beyond the capability of our Titanium Sapphire laser system.

Table I Comparison of the Space position and temperature of the plasmas at the density of $10^{21} \sim 10^{22} \text{ cm}^{-3}$ existed in laser PMMA target interactions for different laser intensity. The time point taken here is 300 ps after the laser pules.

Laser intensity $I \text{ (W/cm}^2\text{)}$	Pulse duration $\tau \text{ (fs)}$	Distance to the target to limit the Region of the plasma at the density of	Electron density of the warm dense matter $T_e \text{ (eV)}$
--	---------------------------------------	--	--

		$10^{21}\sim 10^{22} \text{ cm}^{-3}$	
		$\Delta z (\mu\text{m})$	
10^{13}	100	≤ 1	<0.1
10^{14}	100	<4	<0.7
10^{15}	100	<7	<2
10^{16}	100	<16	<7
5×10^{16}	50	<35	<6

III. Electron density measurement with optical laser interferometry

Optical laser interferometry [5-11] had been verified a convenient, efficient and accurate technique to measure the electron density of plasma generated by short pulse laser. But the capability is limited by two factors: the first one is the so-called critical density and the second is due to the deflection of the probe light in plasma with gradient density [12, 13]. Plasma density higher than $1.7 \times 10^{20} \text{ cm}^{-3}$ had not been reached by using this way up to present. Further more, the measurement should be not very accurate if any deflection exists ineligible. The warm dense matter with electron density of $10^{21}\sim 10^{22} \text{ cm}^{-3}$ then cannot be measured.

However, the gradient tendency of electron density profile (see Figure 2-a) provides an index to search the position of higher density plasma from the lower one. Herein this work, we will measure the profiles of the electron density of the lower density ($<2 \times 10^{20} \text{ cm}^{-3}$) plasma generated by the laser pulse, and then determine the possible position of the warm dense plasma with desire density.

IV. Interferometry Experiments

The pump-probe interferometry experiments were arranged as shown in Figure 3. A single laser pulse with wavelength of 800 nm, pulse duration 50 fs and pulse energy of 3.3 mJ is delivered to an unbalance beam splitter. 99% of the energy of the beam is reflected to a mirror M5 and then focused by a parabola to the planar PMMA target. The diameter is about 10~15 microns as we measured primarily before a real experiment. Hence the laser intensity reached to the target was confidently near 5×10^{16} W/cm². Another 1% part of the beam was frequency doubled by a BBO, and then via a time delay line which was composed of two mirrors M1 and M2, and finally was reflected and sent to the plasma by the two Mirrors M3 and M4. Lens1, Lens 2 and an optical CCD made up a good imaging system to take a microscopy of the small laser-induced plasma with a magnification 10. The Wollaston prism and an additional polarizer

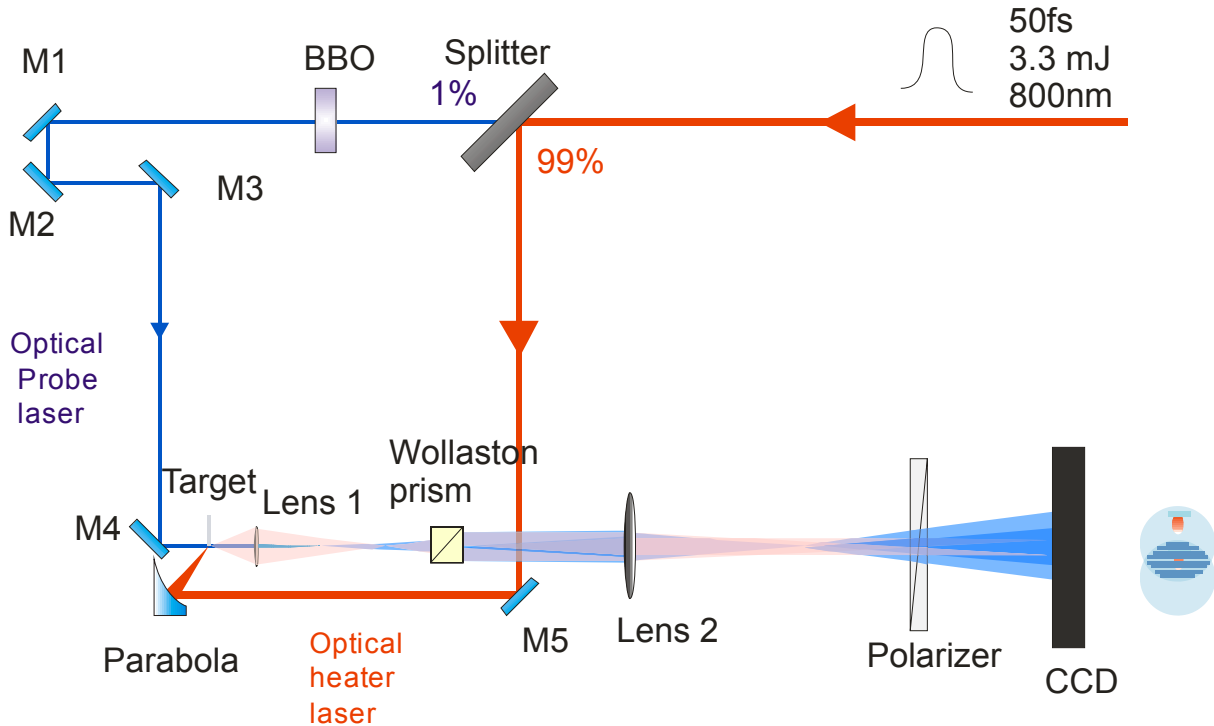


Figure 3. Schematic of the laser plasma interferometry experiments.

which plugged in the light road made the imaging system become a modified Nomarski interferometer. The probe laser including a portion which was distorted by the plasma was split by the Wollaston prism into two beams with perpendicular polarization directions and formed two images on the CCD. The 45° polarizer rotated the two polarized beams into a same polarization direction again and made them interfere each other on the CCD. Notice that the interferometer used here was a little different from the former used one [5]. The modified interferometer here can collect deflected light with larger deflection angle, and hence, can reach higher plasma density. According to Fermat's principle, stronger deflection means steeper density gradient. Further, steeper gradient always is connected with higher density in a laser-induced plasma (please look at Figure 2-a). This modification permits us to reach higher plasma density but unfortunately can lead to some measurement error [14].

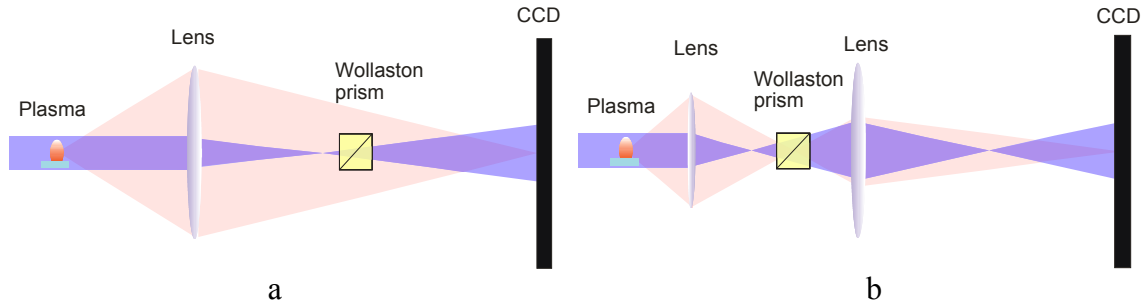


Figure 4. Modification of the interferometer: a). former used Nomarski interferometer in other place; b). presently used interferometer here in this work. The latter one has a larger acceptance solid angle and then can collect stronger deflection light.

V. Results and analysis

Pump-probe experiments had been repeated for lots of times in different time delay (see Figure 2-a) aimed to get a time resolved measurement. We could not get any plasma information when took time delays less than 40 ps. The six interfergram obtained with longer delay time than 40 ps were listed in Figure 5. All the images in Figure 5 had been reconstructed and listed in

Figure 6. These reconstructions were performed by specially developed software for interfergram analysis from Pisa, Italy [15].

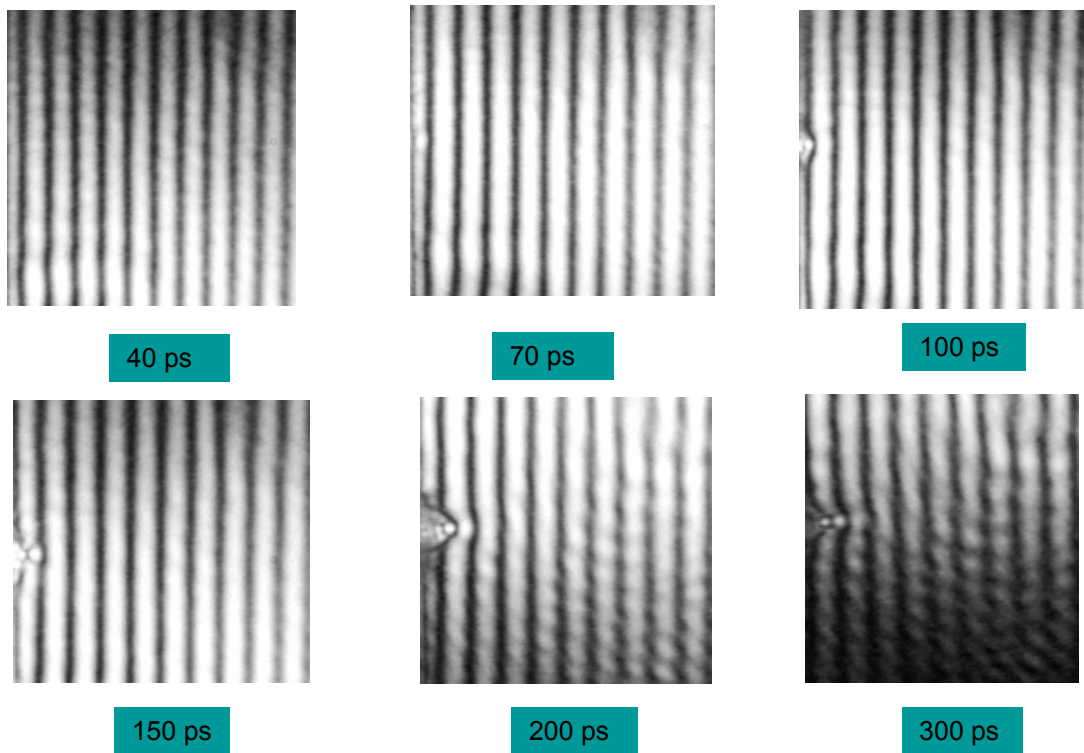


Figure 5. Interfergram obtained in different experiments for different time delay.

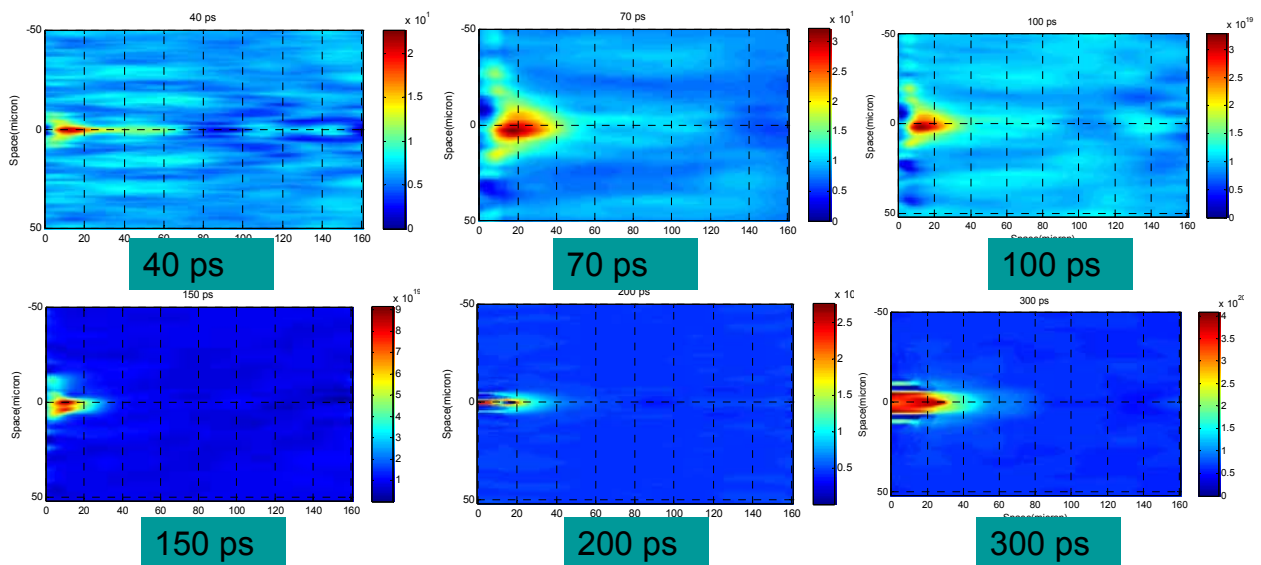


Figure 6. analysis of the interfergram in Figure 5 .

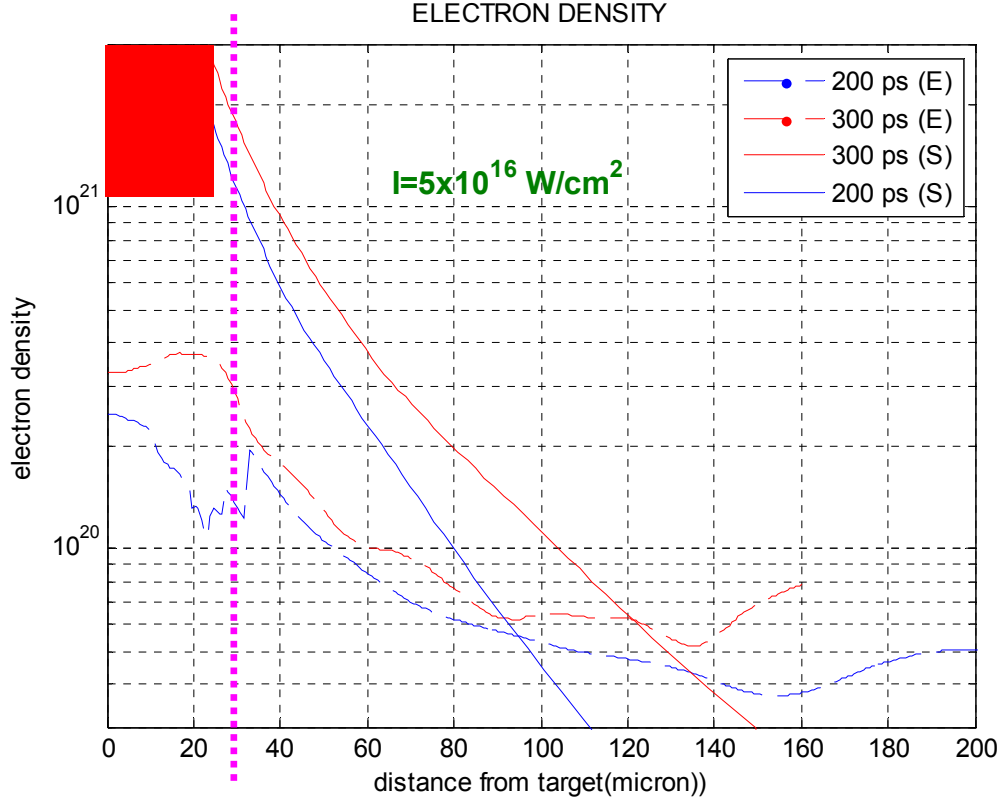


Figure 7. Electron density profiles of the laser-induced along the axis perpendicular to the target. The solid lines give the numerical results while the dashed lines denote the experimental results. The red and the blue lines response to 300 ps and 200 ps time delay respectively.

Figure 7 shows the electron density profiles along the axis perpendicular the target. The experimental curves can be divided into two parts in space. The first part is closed to the target and the distance to the target is not more 30 microns, the second is farer and the distance is great than 30 microns. The first part cannot reflect the truth density profile of the plasma at that region because the gradient there is too steep. In the second part, the curves varied slowly and flatly up to an electron density near to $2 \times 10^{20} \text{ cm}^{-3}$. Judging by the gradient tendency of these curves on can expect that the dense matter should exist at a region where the distance to the target is less than 25 microns.

Agreement between the experiments and the simulations could be found from Figure 7, but obviously there exist some difference. Several possible factors could be the reason which

result it: first of all, the laser parameters we take in the simulation might not so exactly fulfill the practical case; secondly, there could be some errors when we try to find the edges of the target from the experimental data; thirdly and most importantly, according to an previously introduction [14], when deflection of the probe light exists, relevant error similar as the difference in Figure 7 could not be avoided.

VI. Conclusion

Interaction of ultra-short pulse laser and flat PMMA target has been investigated numerically and experimentally. Numerical results show that, the warm dense matter can be found in a region of $z < 35 \mu\text{m}$, at the time 300 ps after the laser beam pulse with parameters of 50 fs in duration, $5 \times 10^{16} \text{ cm}^{-3}$ in intensity and 800 nm in wavelength. Experimental results show that, the dense matter can be expected in a region of $z < 25 \mu\text{m}$, at the time 300 ps after the laser beam pulse (50fs, 3.3J, 10~15 μm in focus diameter). According to such results, we think that laser induced PMMA plasma reaches warm dense matter conditions to be diagnosed by Thomson diagnostics on the FLASH FEL.

VII. Acknowledgement

We gratefully thanks Dr. P. Tomassini who provided us the software to analysis the interfergram, Mr. U. Zastra and Ms. H. Marschner who gave helps in the experiments and Mr. K. U. Amthor whose valuable discussions are helpful and important.

This work was performed under the auspices of the **Virtual Institute VH-VI-104 Plasma Physics Research Using FEL Radiation** of the Helmholtz Society. Supported by the SFB 652 *Strong Correlations and Collective Phenomena in Radiation Fields: Coulomb Systems, Clusters, and Particles*, LDRD 05-ERI-003, and the Alexander von Humboldt Foundation. Work

of O. L. Landen and S. H. Glenzer was performed under the auspices of the U.S. Department of Energy by University of California Lawrence Livermore National Laboratory under contract No. W-7405-Eng-48.

VIII. Reference

1. A. Höll, *et al.*, Internal workshop, Virtual Institute VH-VI-104, Hamburg (13. 02. 2006).
2. R. Redmer, *et al.* Theory of x-ray Thomson scattering in dense plasma, IEEE transactions on plasma science, Vol. 33, 73-84 (2005)
3. A. Höll, *et al.* Pump-probe Thomson scattering at the DESY FEL, 26th international workshop on physics of high energy density in matter, Hirschegg, Austria, 29. 01. 2006~03. 02. 2006
4. A. Djaoui, A user guide for the laser-plasma simulation code: MED 103. Rutherford Appleton Laboratory, 1996.
5. R. Benattar, *et al.*, Polarized light interferometer for laser fusion studies, Rev. Sci. Instrum., Vol. 50, 1853 (1979)
6. Hariharan, P., Optical Interferometry, New York: Academic Press, (2003)
7. H. Schittenhelm, *et al.*, Two-wavelength interferometry on excimer laser induced vapour/plasma plumes during the laser pulse. Applied. Surface. Science, 1998, Vol. 129, 922 (1998)
8. R. E. Walkup, *et al.*, Studies of excimer laser ablation of solids using a Michelson interferometer, Appl. Phys. Lett. Vol. 48, 1690 (1986)
9. L. A. Doyle, *et al.* Three-dimensional electron number densities in a titanium PLD plasma using interferometry, IEEE transactions on plasma science, Vol. 27, 128 (1999)

10. M. Villagran- Muniz, et al, Shadowgraphy and interferometry using a CW laser and a CCD of laser-induced plasma in atmospheric air. IEEE transactions on plasma science, Vol. 77 2464 (2000)
11. S. M. Mao, et al, initiation of a early stage plasma during picosecond laser ablation of solids, Appl. phys. lett. Vol. 77, 2464 (2000)
12. I. V. lisitsyn, et al, effect of laser beam deflection on the accuracy of interferometer measurements, Rev. Sci. Instrum. Vol. 69, 1584 (1998)
13. M. Born and E. Wolf, Principles, Pergamon, Oxford (1964)
14. D. W. Sweeney, et al, Interferometric probing of laser produced plasmas. In: Applied Optics Vol.15, 1126 (1976)
15. P. Tomassini, et al, Application of novel techniques for interferogram analysis to laser–plasma femtosecond probing, Laser and Particle Beams, Vol. 20, 195 (2002).